Published in final edited form as:
J Comp Neurol. 2009 January 10; 512(2): 271–281. doi:10.1002/cne.21882.

Three-Dimensional Reconstruction of the Amphid Sensilla in the Microbial Feeding Nematode, *Acrobeles complexus* (Nematoda: Rhabditida)

Daniel J. Bumbarger[1,*], **Sitara Wijeratne**[1], **Cale Carter**[1], **John Crum**[2], **Mark H. Ellisman**[2], and **James G. Baldwin**[1]

[1]Department of Nematology, University of California, Riverside, California 92521

[2]National Center for Microscopy and Imaging Research, University of California, San Diego, La Jolla, California 92063

Abstract

Amphid sensilla are the primary olfactory, chemoreceptive, and thermoreceptive organs in nematodes. Their function is well described for the model organism *Caenorhabditis elegans*, but it is not clear to what extent we can generalize these findings to distantly related nematodes of medical, economic, and agricultural importance. Current detailed descriptions of anatomy and sensory function are limited to nematodes that recent molecular phylogenies would place in the same taxonomic family, the Rhabditidae. Using serial thin-section transmission electron microscopy, we reconstructed the anatomy of the amphid sensilla in the more distantly related nematode, *Acrobeles complexus* (Cephalobidae). Amphid structure is broadly conserved in number and arrangement of cells. Details of cell anatomy differ, particularly for the sensory neurite termini. We identify an additional sensory neuron not found in the amphid of *C. elegans* and propose homology with the *C. elegans* interneuron AUA. Hypotheses of homology for the remaining sensory neurons are also proposed based on comparisons between *C. elegans*, *Strongyloides stercoralis*, and *Haemonchus contortus*.

Indexing terms

3D-visualization; *Acrobeles complexus*; *Caenorhabditis elegans*; Cephalobina; sensory anatomy; transmission electron microscopy

Early in the development of *Caenorhabditis elegans* as a model organism, the anatomy of the nematode's primary sensory organs, the amphids, was described in considerable detail (Ward et al., 1975; Ware et al., 1975). Amphids are paired lateral sensory structures at the anterior end of the worm, typically composed of 12 or 13 sensory neurites and two support cells each. Subsequent work has dissected the behavioral function of individual amphid neurites and their associated neural networks in considerable detail (e.g., Perkins et al., 1986; Mori and Ohshima, 1995; Chang et al., 2006; Chalasani et al., 2008). Additional anatomical descriptions based on serial section transmission electron microscopy (Ashton et al., 1995; Li et al., 2000a, 2001) and functional studies using laser cell ablation (Ashton et al., 1998, 2007; Li et al., 2000b; Bhopale et al., 2001; Forbes et al., 2004; Ketschek et al., 2004; Nolan et al., 2004) have been conducted in the vertebrate parasites *Strongyloides stercoralis*, *Haemonchus contortus*, and

*Current address and correspondence to: Daniel J. Bumbarger, Department of Evolutionary Biology, Max Planck Institute for Developmental Biology, Spemannstrasse 37/IV, 72076 Tübingen, Germany. daniel.bumbarger@tuebingen.mpg.de.

Ancylostoma caninum. Although classified in the order Strongylida, molecular phylogenies (Kiontke and Fitch, 2005; Meldal et al., 2007) place them in the family Rhabditidae, to which *C. elegans* also belongs. This clade represents just a small portion of nematode biodiversity and it is not clear how much we can generalize these findings to more distantly related nematodes of economic, health, and agricultural importance. Homologs for most individual amphid neurons were identifiable between these three taxa, and in most instances evaluated, the basic function of each neurite examined is phylogenetically conserved.

In an effort to expand our understanding of nematode sensory function, we have described the anatomy of a more distantly related nematode, *Acrobeles complexus*, a globally distributed microbial feeding species in the family Cephalobidae (Cephalobomorpha). This family and its infraorder are closely related to the Tylenchomorpha, a group that includes the majority of the plant parasitic nematode species. It is easier to culture and study than parasitic forms, and as such represents a good platform for extending our knowledge of sensory function in the model organism *C. elegans* to more distantly related groups.

Herein we describe the anatomy of the amphids of adult hermaphrodite and first-stage juveniles of *A. complexus*. We constructed a 3D computer model of the adult hermaphrodite amphid in order to examine details of cell shape that likely correlate with functional differences between taxa. Hypotheses of homology are proposed for individual cells between *A. complexus*, *C. elegans*, *S. stercoralis*, and *H. contortus*.

Materials and Methods

Acrobeles complexus strain jb-132 was cultured on water agar with 0.02 mg/mL cholesterol. Bacteria transferred with the worms multiplied sufficiently to act as a food source. Copper specimen carriers were filled to capacity with nematodes and frozen with a Bal-Tec (Balzers, Liechtenstein) HPM 010 high-pressure freezing apparatus. Freeze substitution was carried out in acetone with 4% osmium tetroxide and 1% uranyl acetate using a Reichert (Depew, NY) CS Auto freeze-substitution apparatus. Specimen carriers were placed in custom chambers to prevent specimen loss (Bumbarger et al., 2006) and were then embedded in slide shaped resin molds (Giammara and Hanker, 1986) using Pelco (Clovis, CA) Eponate-12 embedding media. Individuals were observed first under the light microscope to check specimen preservation, then cut from the epoxy resin slide with a rotary cutting tool and either reembedded in a conventional block mold or attached to empty blocks with cyanoacrylate adhesive with the specimen in an appropriate orientation.

Serial sections ≈75 nm thick were obtained on a Sorvall (Wilmington, DE) MT6000 ultramicrotome and collected on pioloform films fixed to Synaptek wide slot grids. Sections were poststained with methanolic uranyl acetate and lead citrate.

Material was observed with a Phillips (Mahwah, NJ) Tecnai 12 transmission electron microscope operating at 120 KV at the Center for Advanced Microscopy and Microanalysis at the University of California, Riverside. Montaged digital images were taken with a Gatan (Pleasanton, CA) US1000 camera.

Four specimens were examined, each with two amphids. Two adult females were sectioned transversely, one adult female was sectioned longitudinally, and one first-stage juvenile was sectioned transversely.

Tiff image stacks were produced using ImageJ (http://rsb.info.nih.gov/ij/) and then imported into the Imod software package (Kremer et al., 1996) for contour-based volume segmentation and meshing. Mesh models for individual cells were exported in the vrml file format. Errors in the mesh were fixed and both still images and movies were rendered with Blender 2.37

(www.blender3d.org). Figures were finalized, including adjustments to contrast and brightness, in Adobe Photoshop (San Jose, CA) CS3.

Results

The amphid of *Acrobeles complexus* consists of 13 sensory neurons (Figs. 1–3), 12 of which enter a sensory channel formed proximally by a sheath cell and distally by a socket cell. The amphid is ≈15 μm long, as measured from the sensory channel opening in the cuticle to the adherens junctions where the sensory neurites enter the socket cell. The sensory channel exits to the outside environment through an opening between the HypD and HypE epidermal cells and the body wall cuticle.

The anterior sensory channel is lined by cuticle and formed by a self-junction of the socket cell (Fig. 4A). There are no self-junctions in the sheath cell. All dendrites entering the sensory channel do so through a common opening in the sheath cell (Fig. 1C). Near the transition zones of the sensory cilia a small number of lamellar invaginations of the sheath cell membrane occur in the sensory channel. At the point where the sensory dendrite ASK enters the sensory channel, multiple lamellar projections of the sheath cell wrap around the dendrite (Figs. 1B, 4G). Electron transparent vesicles surround this region.

The anterior region of the sheath cell contains a variable number of relatively electron-transparent vesicles, some of which fuse with the membrane forming the sensory channel. One individual represents an extreme version of this feature, with the sensory channel greatly enlarged in both the left and right amphids, presumably by the product contained in these vesicles (Fig. 4F,G).

The 12 neurites that enter the sensory channel have either one or two sensory cilia. All neurites that enter the sensory channel form cilia just distal to the band of adherens junctions. The transition zone of these cilia consists of an outer ring of nine microtubule doublets (Fig. 4B). Radial arms extending interior from each doublet terminate in singlet microtubules. Distal to the transition zone single microtubules extend toward the sensory opening in the cuticle. All amphid cilia have rootlets proximal to the transition zone, although they are generally not robust and sometimes difficult to observe. The arrangement of cell processes is shown in transverse sections at various points in the sensory channel of the sheath cell (Fig. 1). The morphology of individual neurites is variable, particularly proximal to the transition zone. Only features that are observed in multiple amphids are discussed.

Names for neurites in *A. complexus* are based on the position in the sensory channel compared to *S. stercoralis*, the closest relative of *A. complexus* for which data are available.

Five sensory neurites, here named ASB, ASG, ASH, and ASJ, have a simple morphology with a single cilium terminating near the amphid opening. The neurite ASA enters a belt of adherens junctions with the other neurites, but does not form a cilium or project significantly into the sensory channel (Figs. 1A–C, 4H). It forms a junction with the sheath cell for a longer segment than other cells (Fig. 4H). Although it lacks a well-organized cilium, it does express a ciliary rootlet (Fig. 4H) and at the tip expresses a ring-like structure consistent with being a partially formed transition zone. ADC forms two cilia (Figs. 1E, 3C), with the one further from the pharynx having a more prominent swelling near the transition zone (Fig. 3E). Proximal to entering the sheath cell, AFD exhibits a prominent swelling. Distal to adherens junctions with the sheath cell it forms a bulbous swelling of the cell membrane, from which originate 400–500 microvilli and two sensory cilia that terminate in the sensory channel (Figs. 1B–D, 2, 3A, 4E,H). In the center of this swelling the cytosol has a granular appearance. One or more mitochondria are also located in the swelling (Fig. 1B). Microvilli have a prominent actin cytoskeleton and a cell membrane that stains more clearly than surrounding cells (Fig. 4C).

Osmophilic patches in the cytosol associate with the cell membrane and are not found elsewhere in the cell. Many of the microvilli terminate in pockets of the sheath cell, while others terminate between dendrites in the sensory channel. AFD and its associated microvilli are situated ventral to the sensory channel (Figs. 1B–D, 2). ASE has a globular swelling proximal to the transition zone (Fig. 3D). This swelling rests between the two cilia of ADC (Fig. 2). ASF expresses a globular swelling just proximal to the transition zone. From this swelling extends the cilium as well as a short accessory process that terminates in a pocket of the sheath cell (Figs. 2, 3A). Proximal to the band of adherens at the posterior opening of the sheath cell, ASF exhibits a lamellar morphology that wraps partially around ASI. ASI expresses a prominent swelling in the sensory channel, proximal to the transition zone, from which extend multiple finger-like extensions (Fig. 3F). These do not have the distinctive cell membrane found in those of AFD. Proximal to entering the sheath cell, ASI neurites have an accessory process of highly variable morphology. In the individual used to produce the 3D model, ASK has a simple morphology on the left side, but expresses multiple lamellar processes in the sensory channel proximal to the transition zone in the right side, essentially filling in the gaps between other dendrites. The sample size is too small to infer a consistent asymmetry in morphology. ASL has a single cilium morphology in the sensory channel and has a flattened morphology where it touches the opening of the sheath cell. ASM has a variable morphology with respect to the presence or absence of lamellar processes in the sensory channel proximal to the transition zone. In one amphid ASM was missing, although adherens junctions present in the appropriate location indicate a developmental defect.

The amphid of the first-stage juvenile (J1) is ≈12.5 μm long, as measured from the sensory channel opening in the cuticle to the adherens junctions where the sensory neurites enter the socket cell. All dendrites present in the adult also appear in the J1 (Fig. 5) and are similar in appearance, with a few exceptions. The finger cell AFD has ≈75–100 microvilli embedded in the sheath cell. The membrane of the finger cell microvilli did not have the distinctive appearance as described for the adult. The small projection of ASF that is embedded in the sheath cell in the adult is also observed in the J1. The dendrite ASI in the J1 does not have the highly modified appearance of the adult and lacks the finger-like projections as well as a prominent accessory process. Although highly variable, doublet microtubules generally extend much further anteriad from the transition zone than they do in the adult, with some visible in the region of the sensory channel formed by the socket cell. The sheath cell is less complex where the dendrites enter the sensory channel and from it lamellar projections extend that wrap around ASK.

Discussion

The anatomy of the amphid sensilla in the model organism, *C. elegans*, has been described in detail (Ward et al., 1975; Ware et al., 1975). Homology of individual sensory dendrites is not understood for most other nematodes, hindering our ability to generalize our findings in *C. elegans* to species of medical, agricultural, and ecological importance. Here we describe amphids in the microbial feeding nematode, *A. complexus* (Cephalobidae, Nematoda) and propose hypotheses of homology for individual dendrites, based on the spatial relationships between cells and the details of morphology, with those of *C. elegans* and the parasitic nematodes *S. stercoralis* and *H. contortus*.

A stereotypic spatial arrangement of amphid sensory dendrites at both the anterior and posterior sensory channel openings in the sheath cell has been described for the adult hermaphrodite, J2 (second-stage juvenile) and dauer in *C. elegans* (Albert and Riddle, 1983; Ward et al., 1975; Ware et al., 1975), the J3 of *S. stercoralis* (Ashton et al., 1995), and both the J1 (Li et al., 2000a) and J3 (Li et al., 2001) stages of *H. contortus* (Fig. 6). The relative positions of dendrites within the amphid neuron bundle are consistent between individuals. Laser ablation studies

have shown that the general function of individual amphid dendrites is in some cases conserved between animals that are separated by hundreds of millions of years of evolution (Ashton et al., 1998, 2007; Forbes et al., 2004; Ketschek et al., 2004; Nolan et al., 2004). The implication of these observations is that an understanding of amphid cell homology between *C. elegans* and other nematodes can greatly facilitate the study of specific behaviors in distantly related groups.

Individual amphid sensory dendrites can terminate in either a single cilium or paired cilia. The number with paired cilia varies from zero in *S. stercoralis* (Ashton et al., 1995) to three in *H. contortus* (Li et al., 2000a). In *A. complexus* there are two such dual ciliate sensory endings, ADC and the finger cell AFD (Figs. 1E, 3A,E, 4E). The dual ciliate nature of the *A. complexus* finger cell is interesting in the light of similar observations for plant parasitic Tylenchomorpha nematodes (Baldwin and Hirschmann, 1973). *Caenorhabditis elegans, H. contortus,* and *S. stercoralis* all have single ciliate finger cells. Recent phylogenetic studies propose a close relationship between the Tylenchomorpha and the Cephalobmorpha, to which *Acrobeles* belongs (Blaxter et al., 1998; Holterman et al., 2006; Meldal et al., 2007). This may represent a synapomorphy for the clade comprised of these taxa.

Cilia in nematodes differ from those in other phyla in that they are exclusively nonmotile and a fully formed basal body has not been observed. They retain other features, such as a ciliary rootlet and a ring of doublet microtubules, the ciliary necklace (Wright and Carter, 1980; Perkins et al., 1986) anchored to the cell membrane. Perkins et al. (1986) termed these modified basal bodies the transition zone. The amphid cilia of *A. complexus* are very similar to those of *C. elegans*. The transition zone is defined by an outer ring of nine doublet microtubules and an inner ring of singlet microtubules usually found directly opposite each doublet. The morphology of the transition zone has been shown to be variable among nematodes. *Haemonchus contortus* has 10 outer doublet microtubules (Li et al., 2000a), and the plant parasitic nematode, *Heterodera glycines,* has just eight (Endo, 1980). The cilia of another plant parasitic nematode, *Meloidogyne incognita,* can vary between four and seven doublets, depending on the particular sensory neurite (Endo and Wergin, 1977). The much more distantly related nematode, *Xiphinema americanum,* also has nine doublets (Wright and Carter, 1980), and as cilia in most organisms also have nine doublets this is the likely ancestral state for nematodes. The internal ring of singlet microtubules can also be quite variable, with none found in *X. americanum* and only four found in *H. glycines*. The functional consequences of variation in cilium morphology have not been examined. The cytosol inside a cilium is largely compartmentalized from the rest of the cell, and in sensory cilia it may be that microtubules serve primarily to facilitate intraflagellar transport (for review, see Scholey, 2003). The number of microtubules could influence the efficiency of this process.

The finger cell has been shown to have an evolutionary conserved function as a thermoreceptor (Perkins et al., 1986; Li et al., 2000b; Bhopale et al., 2001; Nolan et al., 2004). In *A. complexus* the cell membrane of finger cell microvilli has a distinct appearance as compared to the membrane in other regions of the cell (Fig. 4C). It is possible that they are compartmentalized from the rest of the cell. The microvilli in the J1 of *A. complexus* do not appear to exhibit this modified membrane morphology and thus may differ functionally from the adult.

The position of the finger cell microvilli in relation to the sensory channel has undergone a significant shift within the nematode class Chromadorea. In representatives of this class, *H. contortus* (Li et al., 2000a) and *C. elegans* (Ward et al., 1975), the microvilli are dorsal to the sensory channel, while in *A. complexus* (Figs. 1C, 2) and *S. stercoralis* (Ashton et al., 1995) they are ventral.

The number of dendritic processes entering the amphid differs among these four taxa, with either 12 (*C. elegans* and *H. contortus*) or 13 (*S. stercoralis* and *A. complexus*) (Fig. 6). We propose that the dendrite that accounts for this difference is the homolog of ASA found in both *A. complexus* and *S. stercoralis* (Figs. 1B, 3F, 6). ASA has a distinctive morphology and does not fully enter the sensory channel, terminating instead in the band of adherens junctions at the posterior end of the sheath cell sensory channel (Fig. 4H). Only a small region of the cell membrane is exposed to the outside environment through the sensory channel. Although it does not have a fully formed cilium, it does contain filaments that appear similar to the ciliary rootlets (Fig. 4H) found in other dendrites, and what appears to be a ciliary necklace without microtubules. Interestingly, in a description of the J1 of *H. contortus* (Li et al., 2000a) a dendrite of similar position and morphology is apparent in figures but not discussed, and it is not observable in the J3 (Li et al., 2001).

Although the homolog of the *A. complexus* ASA dendrite is likely not one of those present in the adult *C. elegans* amphid sensory channel, the highly conserved identity of other cells between *A. complexus* and *C. elegans* (Bumbarger et al., 2006, 2007) makes it likely that the cell is present in *C. elegans* but expressed differently and not directly associated with the amphid sheath cell. Amphid anatomy has not been described for the first larval stage of *C. elegans*. It is possible that it follows a similar pattern to *H. contortus*, in which the unnamed homolog of ASA in *A. complexus* is expressed only in the J1 but subsequently is lost from the amphid. AUA, a bilateral pair of dendrites found in the amphid bundle of *C. elegans* but not directly associated with the amphid glial cells (White et al., 1986), is the most likely candidate for an *A. complexus* ASA homolog. AUA in *C. elegans* is known to function in association with social feeding behavior (Coates and de Bono, 2002; Cheung et al., 2004) and as an interneuron involved with oxygen sensation (Chang et al., 2006). These observed functions provide a basis for testing hypotheses of homology proposed here. It may have switched between sensory receptor and interneuron roles and would thus be an interesting study system for understanding the evolution of sensory neuron function. The amphids of *C. elegans* J1 have not been described. It is possible that they are similar to *H. contortus* in having a 13th dendrite only in the J1 stage.

The amphid wing cells AWA, AWB, and AWC dendrites are among the most well-characterized and functionally important sensory dendrites in *C. elegans* (Troemel et al., 1997; L'Etoile and Bargmann, 2000; Bargmann, 2006; Torayama et al., 2007; Chalasani et al., 2008). They are the primary olfactory receptors and are associated with specific chemoattraction and chemorepulsion responses. Despite their importance, it is not well understood what their homologs are in other nematodes. As discussed above, the ASA dendrites in *S. stercoralis* and *A. complexus* are unlikely to be homologs of AWA in *C. elegans*. Assignment of homology is complicated by a more anteriad position for three amphid dendrite nuclei in *S. stercoralis* (Ashton et al., 1995) and the highly derived and elaborate AWA termini in *C. elegans* (Ward et al., 1975) that is not observed in other nematodes.

The sensory cilia of wing cells in *C. elegans* terminate in pockets of the sheath cell rather than in the sensory channel with other sensory dendrites and terminate with high surface area morphology, such as the broad flattened shape of the AWC dendrite (Ward et al., 1975). Only the finger cell exhibits these features in *A. complexus* or *S. stercoralis. Haemonchus contortus* has one additional dendrite, which is embedded in the sheath cell and is a likely homolog of AWC (Li et al., 2000a, 2001). The lack of a similar morphology leaves little to use as a basis for proposing homology for wing cells between *C. elegans* and *A. complexus*. There are two dendrites in *A. complexus* with a modified morphology that represent possible candidates for wing cell homologs. ASF has a single cilium, but just posteriad to the transition zone of this cilium in both the adult and juvenile is a small projection (Figs. 2, 3A) that terminates in a pocket of the sheath cell. Also, the ASI dendrite has multiple finger-like

projections of very fine diameter extending from a swelling proximal to the transition zone (Fig. 3F). Although ASI is modified to have high surface area, these modifications occur proximal to the transition zone rather than distal, as they do in the wing cells of *C. elegans*; thus, it is not considered a likely candidate for homology.

The amphid of one adult individual observed was highly modified. Much of the volume of the sheath cell is filled with large vesicles, and the sensory channel is greatly expanded, presumably filled with secretions from the sheath cell (Fig. 4D,F). This individual may be a mutant phenotype, or it could be responding to an environmental condition different than the other individuals examined, such as starvation or hosting a pathogen. With a small sample size it is not known how common this phenotype is or if it is found in natural populations. It does serve as a reminder that the phenotype of nematode sensory structures can be dynamic. For example, in *C. elegans* the amphid wing cells are known to substantially remodel themselves during the dauer stage, and then, upon emerging from the dauer, returning to a more typical morphology (Albert and Riddle, 1983). *Acrobeles complexus* is often observed to have a sticky secretion surrounding the nose region. Observations made here are consistent with this large amount of secretion product originating from the amphid.

The morphology of the amphid in the J1 of *A. complexus* resembles closely that of the adult. The finger cell is readily identifiable, although the number of microvilli is much smaller. Notably absent are the finger-like projections found on ASI (Fig. 3F). Interestingly, the amphid has a similar length in both the adult and juvenile despite the large difference in body size. The maximal diameter of the amphid is larger in the adult, most likely due to the more elaborate morphology of the adult finger cell.

Patterns of homology between *C. elegans* and other nematodes remain in many cases ambiguous (Fig. 6). In several cases, dendrites that are proposed to be homologs between taxa are likely not (e.g., ASA in *H. contortus* and *C. elegans*). In most cases, including for all of the dendrites in *A. complexus* and most of the dendrites in *S. stercoralis* and *H. contortus*, functional similarity has not been evaluated through, for example, laser ablation studies, leaving us with primarily anatomical similarity for proposing hypotheses of homology. A more complete understanding of homology will require additional functional studies, developmental observations, and an increased taxonomic sampling from which to draw observations. Such work is under way for at least one other nematode, *Pristionchus pacificus* (Ray Hong, pers. commun.). Due to an absence of functional studies, hypotheses of homology for most dendrites in *A. complexus* are particularly poorly understood, and we consider only four classes of dendrites (Fig. 6) to have reasonably clear homologs in other taxa. The finger cell (ADF) has a highly elaborate and phylogenetically conserved anatomy, and its spatial relationships to neighboring dendrites appear also to be conserved. We have discussed earlier the unusual anatomy of ASA. ADC in *A. complexus* shares a double cilium as well as a conserved position in the sensory channel to ADF in *H. contortus*. ASE has a conserved central location in the neurite bundle at the proximal end of the amphid, as well as a conserved position between the two cilia of ADC (in *A. complexus*) and ADF (in *H. contortus*). An absence of modified “wing cell” cilia in *A. complexus*, such as those found in *C. elegans*, is an interesting feature but leads to difficulty in proposing homology. Until hypotheses are more robust we are not recommending a revision of amphid dendrites nomenclature to reflect our understanding of homology.

Acrobeles complexus occupies a convenient phylogenetic position for understanding the evolution of sensory phenotypes and their associated behaviors. It is more closely related to several important vertebrate, insect, and plant parasitic groups than the model organism *C. elegans*. Once patterns of evolution for specific sensory dendrites are more thoroughly

understood, the transfer of information from the model organism *C. elegans* to other lesser known but economically important groups will be more practical.

Acknowledgments

The authors thank Krassimir N. Bozhilov at the Central Facility for Advanced Microscopy and Microanalysis, University of California, Riverside, for support related to TEM image acquisition and an anonymous reviewer for detailed and well-informed criticism of the article.

Grant sponsor: US National Science Foundation; Grant numbers: PEET DEB-9712355, DEB-0731516, and TOL DEB-0228692; Grant sponsor: United States Department of Agriculture; Grant number: 2005-00903.

Literature Cited

Albert PS, Riddle DL. Developmental alterations in sensory neuroanatomy of the *Caenorhabditis elegans* dauer larva. J Comp Neurol 1983;219:461–481. [PubMed: 6643716]

Ashton FT, Bhopale VM, Fine AE, Schad GA. Sensory neuroanatomy of a skin-penetrating nematode parasite: *Strongyloides stercoralis*. I. Amphidial neurons. J Comp Neurol 1995;357:281–295. [PubMed: 7665730]

Ashton FT, Bhopale VM, Holt D, Smith G, Schad GA. Developmental switching in the parasitic nematode *Strongyloides stercoralis* is controlled by the ASF and ASI amphidial neurons. J Parasitol 1998;84:691–695. [PubMed: 9714195]

Ashton FT, Zhu X, Boston R, Lok JB, Schad GA. *Strongyloides stercoralis*: amphidial neuron pair ASJ triggers significant resumption of development by infective larvae under host-mimicking in vitro conditions. Exp Parasitol 2007;115:92–97. [PubMed: 17067579]

Baldwin JG, Hirschmann H. Fine structure of cephalic sense organs in *Meloidogyne incognita* males. J Nematol 1973;5:285–302. [PubMed: 19319352]

Bargmann, CI. Chemosensation in *C. elegans*. In: WormBook. , editor. The C. elegans Research Community, WormBook; 2006. http://www.wormbook.org

Bhopale VM, Kupprion EK, Ashton FT, Boston R, Schad GA. *Ancylostoma caninum*: the finger cell neurons mediate thermotactic behavior by infective larvae of the dog hookworm. Exp Parasitol 2001;97:70–76. [PubMed: 11281703]

Blaxter ML, DeLey P, Garey JR, Liu LX, Scheldeman P, Vierstraete A, Vanfleteren JR, Mackey LY, Dorris M, Frisse LM, Vida JT, Thomas WK. A molecular evolutionary framework for the phylum Nematoda. Nature 1998;392:71–75. [PubMed: 9510248]

Bumbarger DJ, Crum J, Ellisman MH, Baldwin JG. Three-dimensional reconstruction of the nose epidermal cells in the microbial feeding nematode, *Acrobeles complexus* (Nematoda: Rhabditida). J Morphol 2006;267:1257–1272. [PubMed: 16710857]

Bumbarger DJ, Crum J, Ellisman MH, Baldwin JG. Three-dimensional fine structural reconstruction of the nose sensory structures of Acrobeles complexus compared to *Caenorhabditis elegans* (Nematoda: Rhabditida). J Morphol 2007;268:649–663. [PubMed: 17514723]

Chalasani SH, Chronis N, Tsunozaki M, Gray JM, Ramot D, Goodman MB, Bargmann CI. Dissecting a circuit for olfactory behaviour in *Caenorhabditis elegans*. Nature 2008;451:102.

Chang AJ, Chronis N, Karow DS, Marletta MA, Bargmann CI. A distributed chemosensory circuit for oxygen preference in *C. elegans*. PLoS Biol 2006;4:e274. [PubMed: 16903785]

Cheung BH, Arellano-Carbajal F, Rybicki I, de Bono M. Soluble guanylate cyclases act in neurons exposed to the body fluid to promote *C. elegans* aggregation behavior. Curr Biol 2004;14:1105–1111. [PubMed: 15203005]

Coates JC, de Bono M. Antagonistic pathways in neurons exposed to body fluid regulate social feeding in *Caenorhabditis elegans*. Nature 2002;419:925–929. [PubMed: 12410311]

Endo BY. Ultrastructure of the anterior neurosensory organs of the larvae of the soybean cyst nematode, *Heterodera glycines*. J Ultrastruct Res 1980;72:349–366. [PubMed: 7191907]

Endo BY, Wergin WP. Ultrastructure of anterior sensory organs of the root-knot nematode, *Meloidogyne incognita*. J Ultrastruct Res 1977;59:231–249. [PubMed: 864822]

Forbes WM, Ashton FT, Boston R, Zhu X, Schad GA. Chemoattraction and chemorepulsion of *Strongyloides stercoralis* infective larvae on a sodium chloride gradient is mediated by amphidial neuron pairs ASE and ASH, respectively. Vet Parasitol 2004;120:189–198. [PubMed: 15041094]

Giammara BL, Hanker JS. Epoxy-slide embedment of cytochemically stained tissues and cultured cells for light and electron microscopy. Stain Technol 1986;61:51–58. [PubMed: 2420040]

Holterman M, van der Wurff A, van den Elsen S, van Megen H, Bongers T, Holovachov O, Bakker J, Helder J. Phylum-wide analysis of SSU rDNA reveals deep phylogenetic relationships among nematodes and accelerated evolution toward crown clades. Mol Biol Evol 2006;23:1792–1800. [PubMed: 16790472]

Ketschek AR, Joseph R, Boston R, Ashton FT, Schad GA. Amphidial neurons ADL and ASH initiate sodium dodecyl sulphate avoidance responses in the infective larva of the dog hookworm *Anclyostoma caninum*. Int J Parasitol 2004;34:1333–1336. [PubMed: 15542093]

Kiontke K, Fitch DH. The phylogenetic relationships of *Caenorhabditis* and other rhabditids. WormBook 2005:1–11. [PubMed: 18050394]

Kremer JR, Mastronarde DN, McIntosh JR. Computer visualization of three-dimensional image data using IMOD. J Struct Biol 1996;116:71–76. [PubMed: 8742726]

L'Etoile ND, Bargmann CI. Olfaction and odor discrimination are mediated by the *C. elegans* guanylyl cyclase ODR-1. Neuron 2000;25:575–586. [PubMed: 10774726]

Li J, Ashton FT, Gamble HR, Schad GA. Sensory neuroanatomy of a passively ingested nematode parasite, *Haemonchus contortus*: amphidial neurons of the first stage larva. J Comp Neurol 2000a; 417:299–314. [PubMed: 10683605]

Li J, Zhu X, Boston R, Ashton FT, Gamble HR, Schad GA. Thermotaxis and thermosensory neurons in infective larvae of *Haemonchus contortus*, a passively ingested nematode parasite. J Comp Neurol 2000b;424:58–73. [PubMed: 10888739]

Li J, Zhu X, Ashton FT, Gamble HR, Schad GA. Sensory neuroanatomy of a passively ingested nematode parasite, *Haemonchus contortus*: Amphidial neurons of the third-stage larva. J Parasitol 2001;87:65–72. [PubMed: 11227904]

Meldal BH, Debenham NJ, De Ley P, De Ley IT, Vanfleteren JR, Vierstraete AR, Bert W, Borgonie G, Moens T, Tyler PA, Austen MC, Blaxter ML, Rogers AD, Lambshead PJ. An improved molecular phylogeny of the Nematoda with special emphasis on marine taxa. Mol Phylogenet Evol 2007;42:622–636. [PubMed: 17084644]

Mori I, Ohshima Y. Neural regulation of thermotaxis in *Caenorhabditis elegans*. Nature 1995;376:344–348. [PubMed: 7630402]

Nolan TJ, Brenes M, Ashton FT, Zhu X, Forbes WM, Boston R, Schad GA. The amphidial neuron pair ALD controls the temperature-sensitive choice of alternative developmental pathways in the parasitic nematode, *Strongyloides stercoralis*. Parasitology 2004;129:753–759. [PubMed: 15648698]

Perkins LA, Hedgecock EM, Thomson JN, Culotti JG. Mutant sensory cilia in the nematode *Caenorhabditis elegans*. Dev Biol 1986;117:456–487. [PubMed: 2428682]

Scholey JM. Intraflagellar transport. Annu Rev Cell Dev Biol 2003;19:423–443. [PubMed: 14570576]

Torayama I, Ishihara T, Katsura I. *Caenorhabditis elegans* integrates the signals of butanone and food to enhance chemotaxis to butanone. J Neurosci 2007;27:741–750. [PubMed: 17251413]

Troemel ER, Kimmel BE, Bargmann CI. Reprogramming chemotaxis responses: sensory neurons define olfactory preferences in *C. elegans*. Cell 1997;91:161–169. [PubMed: 9346234]

Ward S, Thomson N, White JG, Brenner S. Electron microscopical reconstruction of the anterior sensory anatomy of the nematode *Caenorhabditis elegans*. J Comp Neurol 1975;160:313–337. [PubMed: 1112927]

Ware R, Clark D, Crossland K, Russell RL. The nerve ring of the nematode *Caenorhabditis elegans*: Sensory input and motor output. J Comp Neurol 1975;162:71–110.

White JG, Southgate E, Thomson JN, Brenner S. The structure of the nervous system of the nematode *Caenorhabditis elegans*. Philos Trans R Soc Lond B Biol Sci 1986;314:1–340.

Wright KA, Carter R. Cephalic sense organs and body pores of *Xiphinema americanum* (Nematoda: Dorylaimoidea). Can J Zool 1980;58:1439–1451. [PubMed: 7427831]

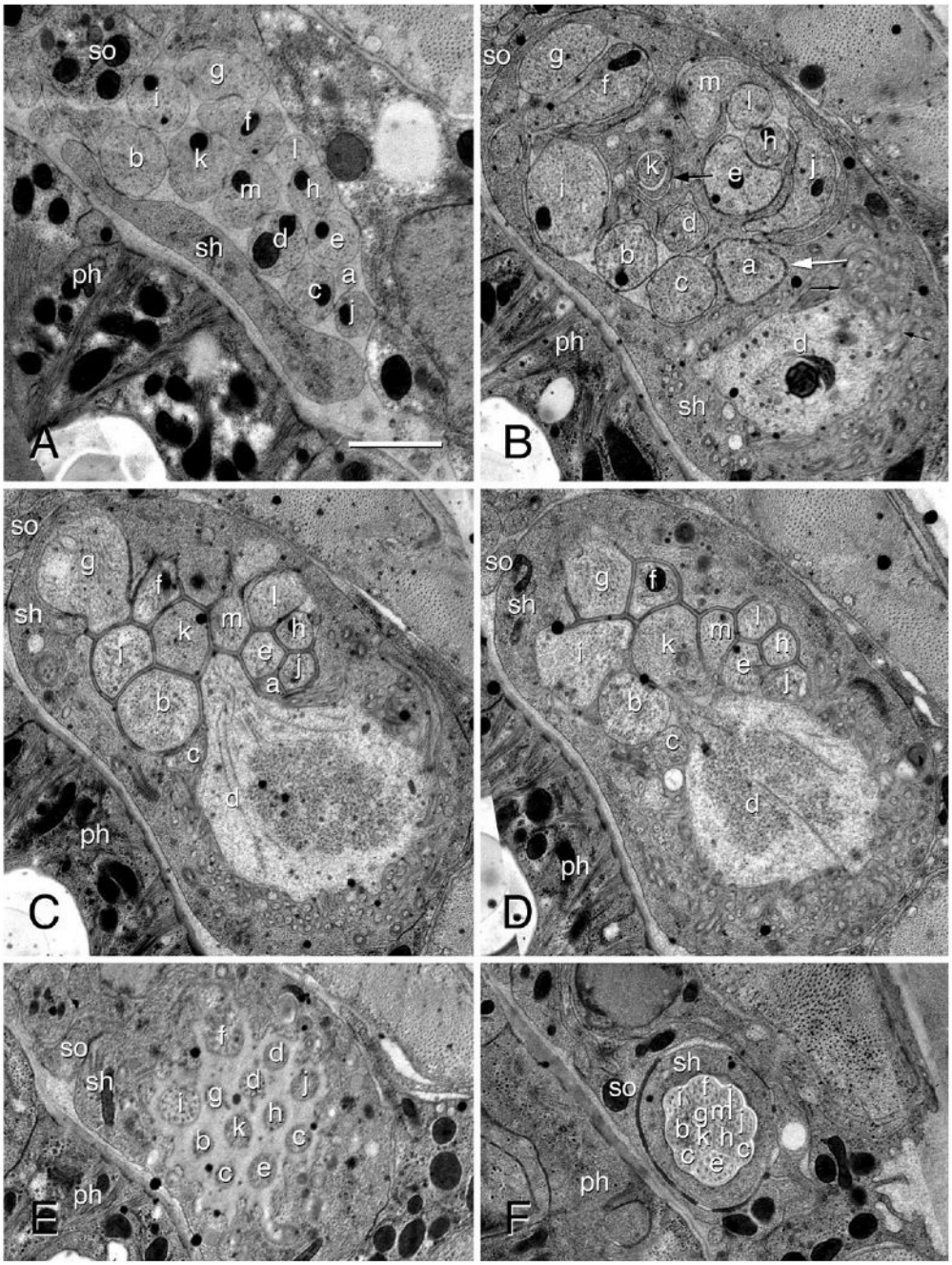

Figure 1.

Transmission electron micrographs of an amphid in an adult female of *Acrobeles complexus*. **A:** The amphid posterior to the expansion of the sheath cell. The sensory dendrites ASA (a), ASB (b), ADC (c), AFD (d), ASE (e), ASF (f), ASG (g), ASH (h), ASI (i), ASJ (j), ASK (k), ASL (l), and ASM (m) are shown. Also indicated are the sheath cell (sh), socket cell (so), and the pharynx (ph). The labels for A apply to all other panels. **B:** The amphid posterior to the entrance of dendrites into the sensory channel formed by the sheath cell. Note coils of lamellar processes formed by the sheath cell (large black arrow) that wrap around the ASK dendritic process. Junctions with a distinct morphology (white arrow) occur between the sheath cell and the dendrite ASA. Microvilli branching off of the AFD dendrite are indicated (small black

arrows). **C:** The belt of adherens junctions between adjacent amphid dendrites and the sheath cell, forming a single opening into the sensory channel. A bulbous extension of AFD extending into the sheath cell, with microvilli branching from this bulb. Note the granular appearance of the cytosol in the center of the bulb. **D:** One of two AFD cilia originating on the bulbous process (white arrow). **E:** The sensory channel of the amphid, showing the transition zones of most sensory amphid dendrites. Note the two cilia of ADC. **F:** Transition between the sheath and socket cells, showing adherens junctions between the two cells. Scale bar = 1 μm (applies to all).

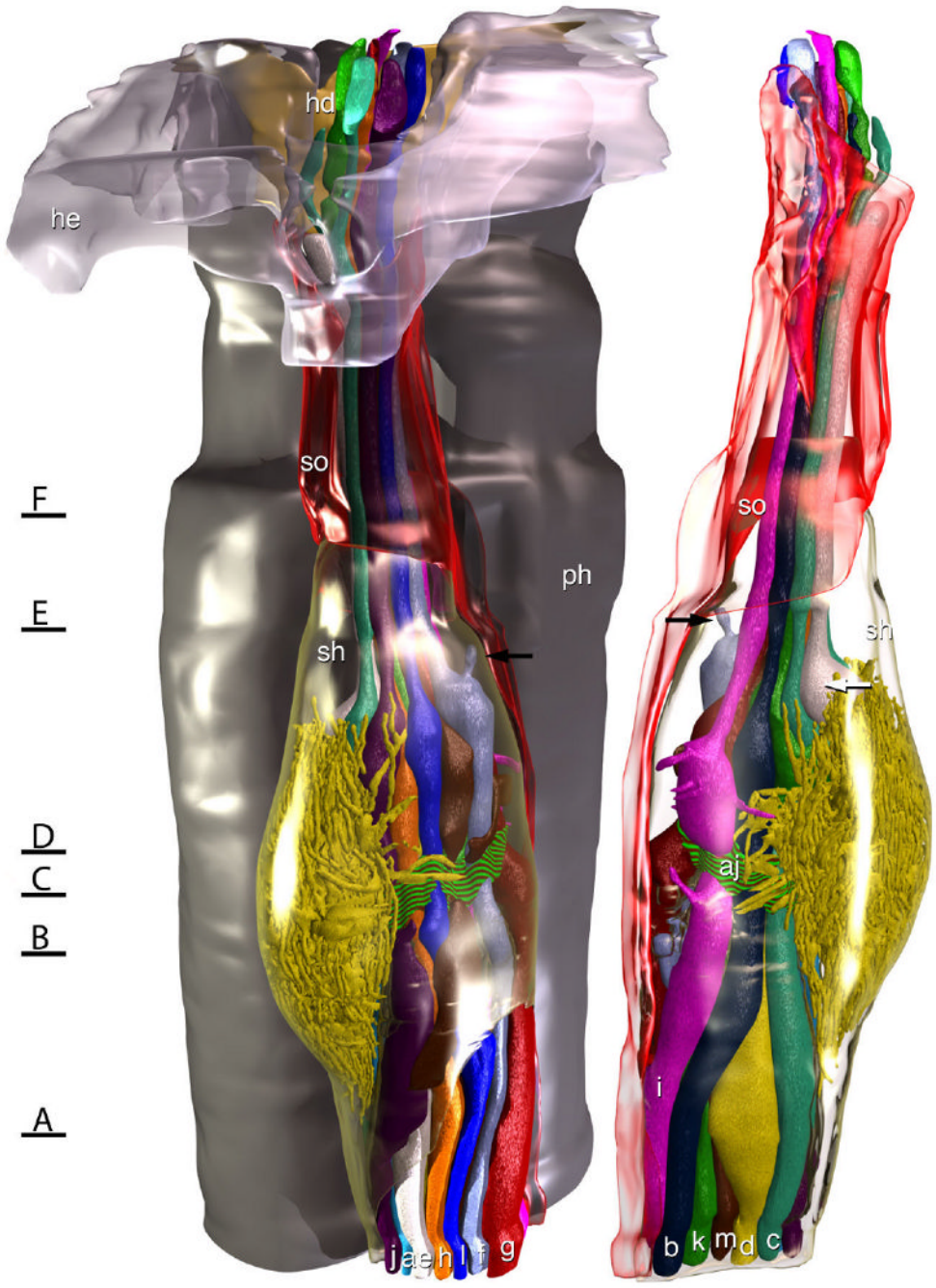

Figure 2.

Model of the amphid of *Acrobeles complexus*. In the rendering on the left the left amphid is viewed from the left side of the animal, and in the rendering on the right the same amphid is viewed from the opposite side. The amphid socket cell (so) is rendered transparent red and the sheath cell (sh) is rendered transparent green. For reference, on the left side a portion of the HYP-E epidermal syncytium (he) is rendered transparent gray and a portion of the HYP-D epidermal syncytium (hd) is rendered solid yellow, showing where they form the amphid opening to the outside environment. Behind the amphid, a portion of the pharynx is rendered in gray. A belt of adherens junctions at the point where dendritic processes enter the sensory channel (aj) is indicated by a red and green striped texture. A small accessory process of ASF

(black arrows) terminates in a pocket of the sheath cell, rather than in the sensory channel of the amphid. The bulbous swelling of ASE (white arrow) rests between the two cilia of ADC. Black lines with letters indicate the approximate region of the amphid from which the images in Figure 1 were obtained.

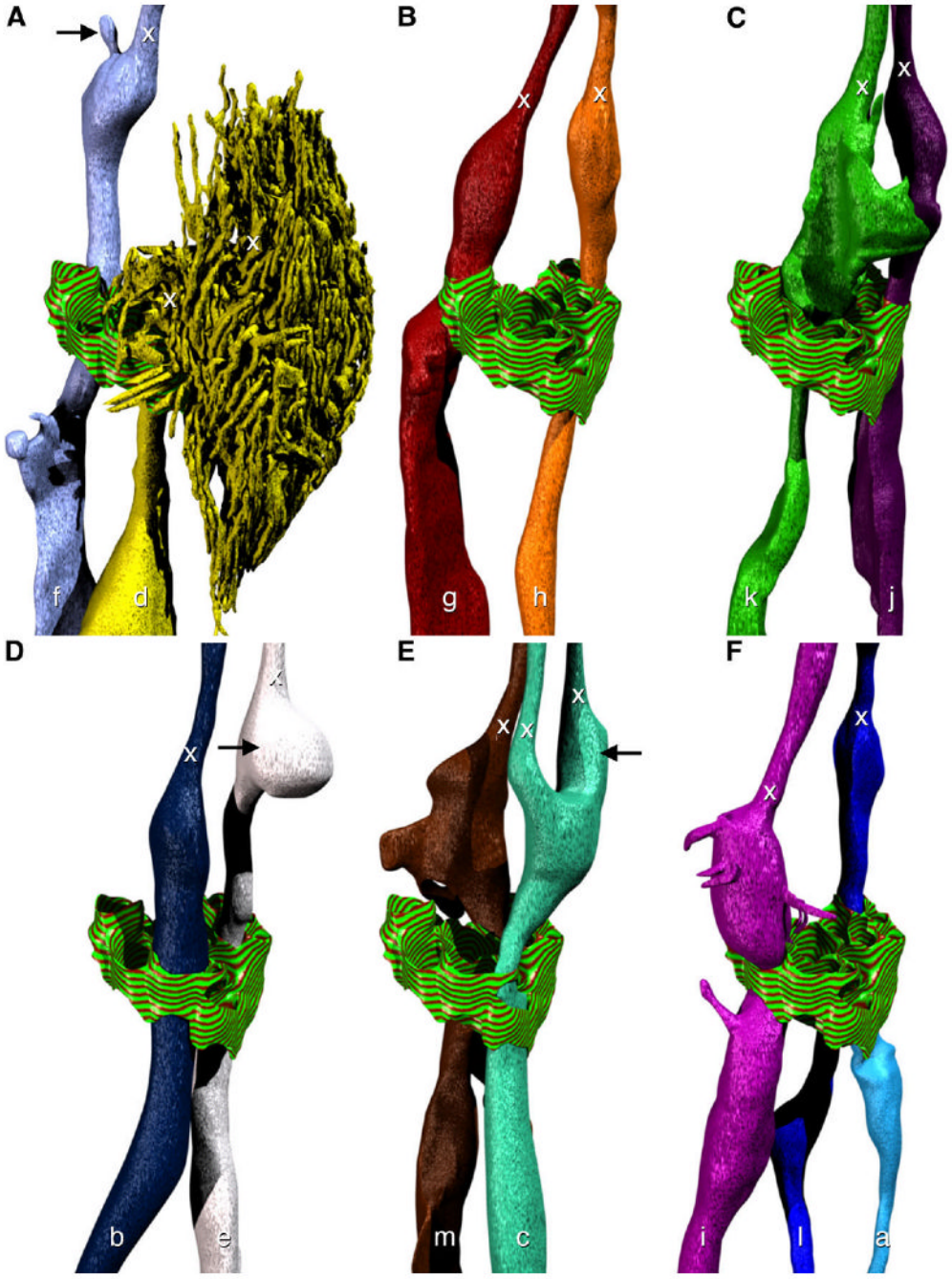

Figure 3.

Model of the morphology of individual amphid dendrites. Adherens junctions at the opening in the sheath cell to the sensory channel are indicated with a striped green and red texture. The positions of transition zones (x) are indicated for all dendrites. The perspective is identical to the right-hand side of Figure 2. **A:** The neurites ASF (f) and ADF (d). Note the small projection (black arrow) near the transition zone. **B:** The neurites ASG (g) and ASH (h). **C:** The neurites ASK (k) and ASJ (j). **D:** The neurites ASB (b) and ASE (e). The bulbous swelling (black arrow) of ASE rests between the two cilia of ADC. **E:** The neurites ASM (m) and ADC (c). The cilium of ADC that is further from the pharynx has a more robust swelling near the transition zone (black arrow). **F:** The neurites ASI (i), ASL (l), and ASA (a).

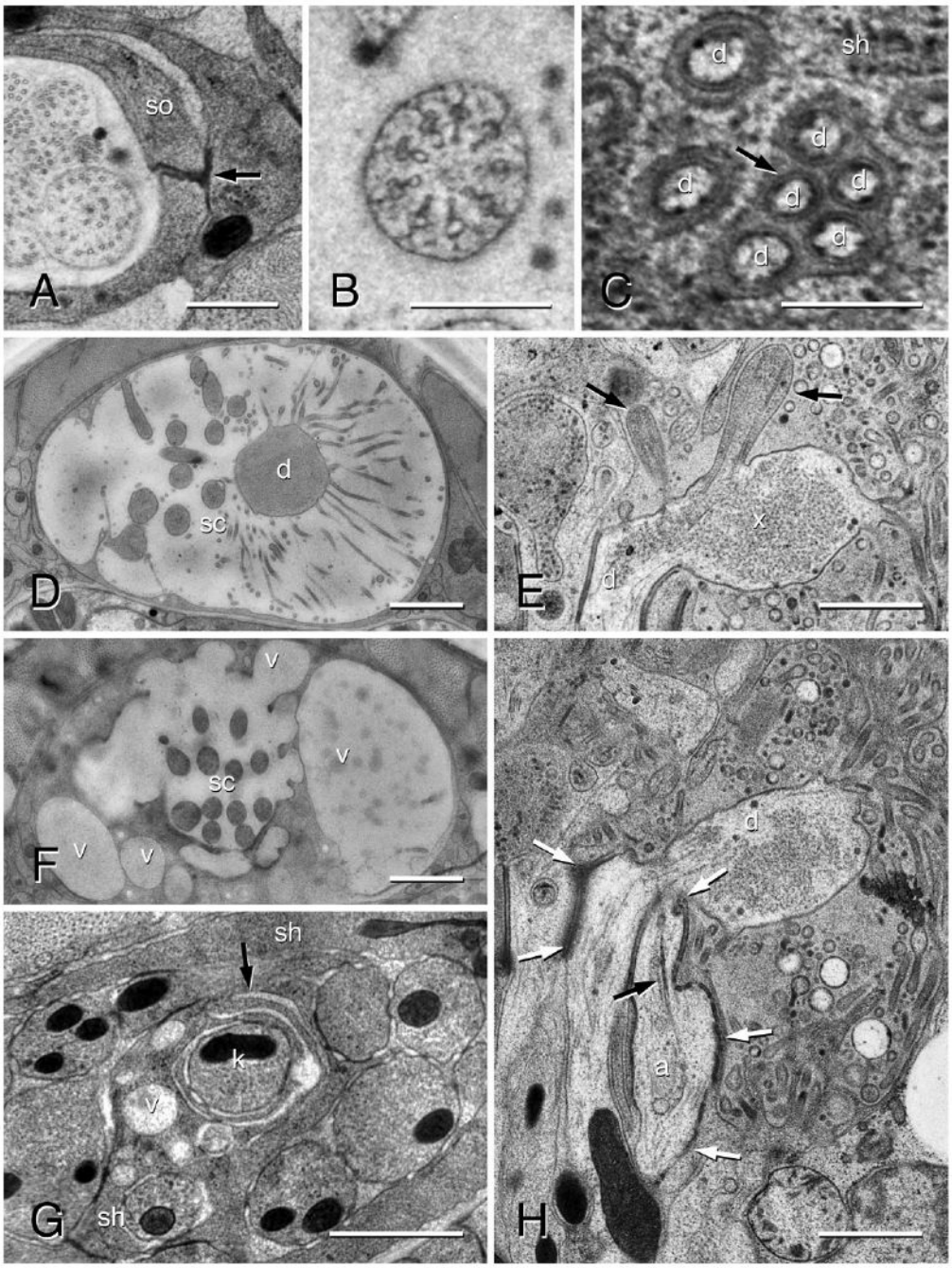

Figure 4.

Transmission electron micrographs of an amphid in an adult female of *Acrobeles complexus*. **A:** Anterior region of amphid sensory channel showing the self-junction (black arrow) of the socket cell (so). **B:** Transition zone of an amphid sensory cilium. **C:** Distinctive cell membranes (black arrow) of the AFD microvilli (d) shown adjacent to the sheath cell (sh) membrane. **D:** Amphid in the region of the AFD (d) microvilli. The amphid sensory channel (sc) in this individual is filled with a secretion from the sheath cell. **E:** Longitudinal image through the amphid finger cell (d) showing two sensory cilia (black arrows) and granular material in the cytosol of the finger cell bulb (x). **F:** The same individual as in D, shown in the anterior region of the sensory channel (sc) where large secretory vesicles (v) merge with the sensory channel.

G: Lamellar projections (black arrow) of the sheath cell (sh) wrapping around the sensory dendrite ASK (k) just posterior to where it enters the sheath cell sensory channel. Note the numerous vesicles (v) in this region. Scale bar = 1 μm. **H:** Longitudinal section through the amphid. The partially formed cilium of ASA (a) is shown terminating adjacent to the AFD cell (d). The rootlet is indicated (black arrow). Note the greater surface area of adherens junctions (white arrows) along ASA as compared to the other sensory dendrites. Scale bars = 0.5 μm in A; 0.25 μm in B,C; 1 μm in D–H.

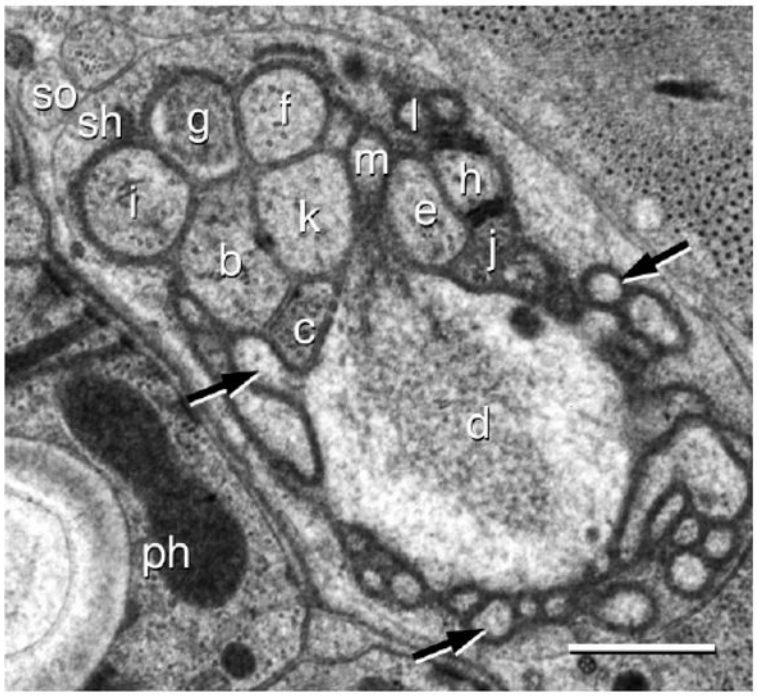

Figure 5.

Transmission electron micrograph of an amphid in the J1 of *Acrobeles complexus*. The sensory dendrites ASB (b), ADC (c), AFD (d), ASE (e), ASF (f), ASG (g), ASH (h), ASI (i), ASJ (j), ASK (k), ASL (l), and ASM (m) are shown at the entrance to the sheath cell sensory channel. Also indicated are the sheath cell (sh), socket cell (so), and the pharynx (ph). The AFD cell is surrounded by microvilli, three of them are indicated (black arrows). Scale bar = 0.5 μm.

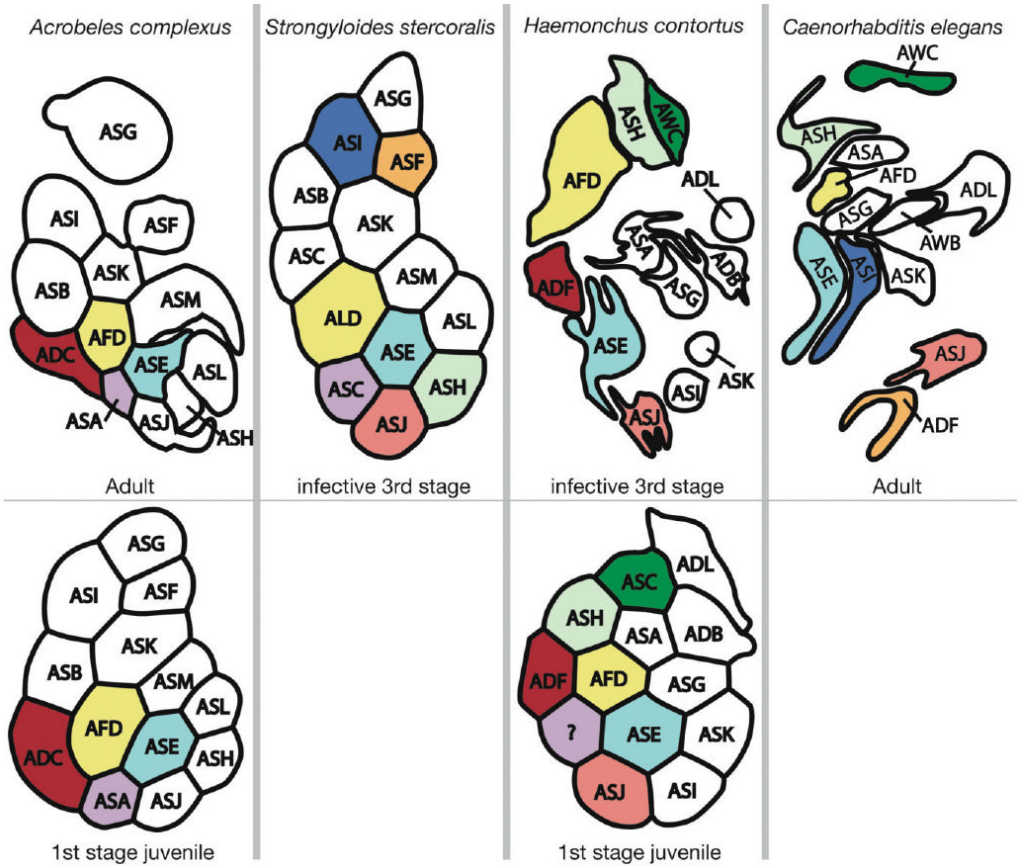

Figure 6.

Arrangement of amphid dendrites at the posterior entrance into the sheath cell. The bottom row is from J1 while the top row is from the oldest life stage for which there is data. The right side of each image is adjacent to the pharynx, and the top is dorsal. Letters correspond to the name of dendrites according to current nomenclature. Cells that are colored the same represent stronger hypotheses of homology that are based on multiple types of similarity, with dendrites of the same color being presumably homologous. Types of similarity considered include number of cilia, results of laser ablation studies that imply related function, and relative position at the proximal end of the amphid. Data for *Strongyloides stercoralis* are redrawn from Ashton et al. (1995). Data for *Haemonchus contortus* are redrawn from Li et al. (2000a, 2001). Data for *C. elegans* are redrawn from Ward et al. (1975).